

# Carbon Abundances of Metal-Poor Stars Determined from the C I 1.068–1.069 $\mu\text{m}$ Lines \* †

Yoichi TAKEDA

*National Astronomical Observatory of Japan 2-21-1 Osawa, Mitaka, Tokyo 181-8588*  
*takeda.yoichi@nao.ac.jp*

and

Masahide TAKADA-HIDAI

*Liberal Arts Education Center, Tokai University, 4-1-1 Kitakaname, Hiratsuka, Kanagawa 259-1292*  
*mth\_tsc@tsc.u-tokai.ac.jp*

(Received 2013 January 7; accepted 2013 January 26)

## Abstract

A non-LTE analysis of C I lines at 1.068–1.069  $\mu\text{m}$  was carried out for selected 46 halo/disk stars covering a wide metallicity range ( $-3.7 \lesssim [\text{Fe}/\text{H}] \lesssim +0.3$ ), based on the spectral data collected with IRCS+AO188 of the Subaru Telescope, in order to examine whether and how these strong neutral carbon lines of multiplet 1 can be exploited for establishing stellar carbon abundances, especially for very metal-poor stars where CH molecular lines have been commonly used. These C I lines were confirmed to be clearly visible for all stars down to  $[\text{Fe}/\text{H}] \sim -3.7$ , from which C abundances could be successfully determined. The resulting  $[\text{C}/\text{Fe}]$  vs.  $[\text{Fe}/\text{H}]$  diagram revealed almost the same trend established from previous studies. When the results for individual stars are compared with the published data collected from various literature, while a reasonable agreement is seen as a whole, a tendency is observed that our abundances are appreciably higher than those from CH lines especially for very metal-poor giants of low gravity. Since the abundances of these C I lines are subject to rather large non-LTE corrections (typically by several tenths dex) whose importance progressively grows as the metallicity is lowered, attention should be paid to how the collisional rates (especially due to neutral hydrogen) are treated in non-LTE calculations.

**Key words:** stars: abundances — stars: atmospheres — stars: late-type  
— stars: Population II

## 1. Introduction

The abundances of carbon (one of the most abundant elements next to hydrogen, helium, and oxygen) play a significant role in stellar spectroscopy. Above all, the behavior of C in the very metal-poor regime ( $[\text{Fe}/\text{H}] \lesssim -2$ ) is important, since various peculiarities (i.e., enhancement as well as deficiency) are observed, which have attracted interest of astrophysicists in the field of galactic nucleosynthesis or stellar evolution. Thus a number of carbon abundance studies of metal-deficient stars have been published so far, as compiled in SAGA<sup>1</sup> (Stellar Abundances for the Galactic Archeology) database (Suda et al. 2008, 2011). Regarding the spectral lines to be invoked for spectroscopically determining the abundance of carbon, several indicators are known to usable, such as atomic lines (C I) or molecular lines (CH, C<sub>2</sub>), each of which have different visibilities depending on the type of stars, and have different characteristics; e.g., in terms of the sensitivity to the 3D effect or non-LTE effect (cf. Asplund 2005; subsection 3.3 therein).

Focusing on very metal-deficient stars in the galactic halo ( $-4 \lesssim [\text{Fe}/\text{H}] \lesssim -2$ ), we note that most studies on carbon abundances have been done based on CH molecular lines in the blue region (G band) which are so strong as to be visible even at such an extremely low metallicity. Although a group of neutral carbon lines at 9061–9111 Å (multiplet 3;  $3s\ ^3\text{P}^\circ - 3p\ ^3\text{P}$ ;  $\chi_{\text{low}} \sim 7.5$  eV) were sometimes used for metal-poor dwarfs by several investigators (Tomkin et al. 1992; Akerman et al. 2004; Takeda & Honda 2005; Fabbian et al. 2006, 2009), they have not been the mainstream (presumably because they may suffer an appreciable non-LTE effect).

Here, we should realize that other C I lines are available in near-IR region, which are namely the lines at  $\sim 1.07$   $\mu\text{m}$  (multiplet 1;  $3s\ ^3\text{P}^\circ - 3p\ ^3\text{D}$ ;  $\chi_{\text{low}} \sim 7.5$  eV) originating from the same lower term ( $3s\ ^3\text{P}^\circ$ ) as multiplet 3 lines. Actually, they are even more suitable than C I 0.91  $\mu\text{m}$  lines, because of their strengths (the transition probability of the strongest C I 10691 line in multiplet 1 is larger by 0.2 dex than the strongest C I 9094.83 line in multiplet 3; cf. table 2) as well as their location in the spectral region almost free from telluric lines (these are actually a nuisance problem for C I 0.91  $\mu\text{m}$  lines). However, to our knowledge, these lines have barely been used for carbon abundance determinations, except for the Sun and Vega (e.g., Stürenburg & Holweger 1990; Takeda 1992, 1994).

\* Based on data collected at Subaru Telescope, which is operated by the National Astronomical Observatory of Japan.

† The large data tables are separately provided in the machine-readable form as electronic tables E1 and E2.

<sup>1</sup> Available on-line at (<http://saga.sci.hokudai.ac.jp/>).

Why not exploit these lines to study carbon abundances of metal-poor stars by making use of these merit?

Timely, we recently obtained near-IR ( $zJ$ -band; 1.04–1.19  $\mu\text{m}$ ) high-dispersion spectra of 46 disk/halo stars (dwarfs as well as giants) in a wide metallicity range ( $-3.7 \lesssim [\text{Fe}/\text{H}] \lesssim +0.3$ ), by using the Subaru Telescope with IRCS+AO188, and carried out sulfur abundance determinations based on the S I triplet lines at 10455–10459  $\text{\AA}$  (Takeda & Takada-Hidai 2011a, 2012; hereinafter referred to as Paper I and Paper II, respectively). We thus decided to study the strong C I lines of multiplet 1 at  $\sim 1.07 \mu\text{m}$  in these spectra, in order to see whether the C abundances of very metal-poor stars can be successfully determined by these lines and how they are compared with the published results derived from other lines (such as those of CH). This is the purpose of this investigation.

The remainder of this article is organized as follows. After describing the observational data in section 2, we explain the details of abundance determinations (stellar parameters, treatment of non-LTE effect, method of analysis, uncertainties, etc.) in section 3. Section 4 is devoted to the discussion section, where the results are examined, compared with the published work, and the merits and problems of these near-IR C I lines are discussed. The summary is given in section 5. In the Appendix, the grid of theoretical non-LTE corrections for the C I 9061–9111 lines of multiplet 3 are re-presented, since a mis-treatment was found in our previously published results.

## 2. Observational Data

The observational data used for this study are the high-dispersion ( $R \sim 20000$ )  $zJ$ -band (1.04–1.19  $\mu\text{m}$ ) spectra obtained by using IRCS+AO188 of the Subaru Telescope in two observing periods of 2009 July 29 and 30 (UT) as well as 2011 August 17 and 18 (UT). In the former 2009 July run, 33 comparatively bright stars of wide varieties (from  $[\text{Fe}/\text{H}] \sim -3.7$  to  $\sim +0.3$ , dwarfs as well as giants) were observed,<sup>2</sup> while selected 13 very metal-poor stars ( $[\text{Fe}/\text{H}] \lesssim -2$ ) and Vesta (substitute for the Sun) were targeted in the latter 2011 August run. This makes 47 ( $= 33 + 13 + 1$ ) spectra as a total, though the net number is 46 because G 64-37 was repeatedly observed. See section 2 of Papers I and II for more details of the observations and the data reduction. The list of these 47 objects is given in table 1, where the targets in 2009 and those in 2011 are separately presented.

The 2009 July spectra for representative 4 stars of different metallicities along with Altair in the 10650–10750  $\text{\AA}$  region are displayed in figure 1. Note that most of the conspicuous lines are those of neutral carbon and silicon, and several strong C I lines (e.g., at 10683, 10691, 10730  $\text{\AA}$ ) are clearly visible also for the most metal-poor star (BD +44 493). Besides, we can recognize from this figure (see the broad-line spectrum of Altair) that this region is practically free from any telluric lines, in contrast

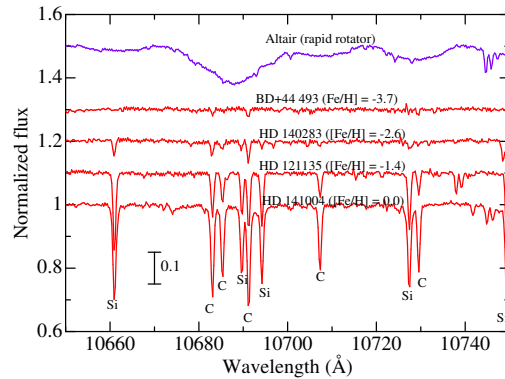


**Fig. 1.** Spectra of representative 4 stars with different metallicities in the 10650–10750  $\text{\AA}$  region comprising C I and Si I lines, where the wavelength scale of stellar lines is adjusted to the laboratory frame. The spectrum of Altair is also shown to demonstrate the negligible effect of telluric lines.

to the C I 9061–9111 region influenced by  $\text{H}_2\text{O}$  lines of earth’s atmosphere origin.

## 3. Abundance Determination

### 3.1. Non-LTE Calculations and Model Atmospheres

Regarding the atmospheric parameters ( $T_{\text{eff}}$ ,  $\log g$ ,  $v_t$ , and  $[\text{Fe}/\text{H}]$ ) of the program stars necessary for constructing model atmospheres and determining abundances, we used exactly the same values as adopted in Papers I and II, in which various published studies were consulted (cf. caption in table 1 of Papers I and II for the individual reference sources). These parameters are presented in table 1.

As to the computation of non-LTE departure coefficients, we closely followed our previous work (see Takeda 1992, 1994; Takeda & Honda 2005 for the details). Practically, our non-LTE calculations were carried out on a large grid of 150 ( $= 6 \times 5 \times 5$ ) models corresponding to combinations of six  $T_{\text{eff}}$  (4500, 5000, 5500, 6000, 6500, 7000 K), five  $\log g$  (1, 2, 3, 4, 5), and five  $[\text{Fe}/\text{H}]$  ( $-4, -3, -2, -1, 0$ ), where  $[\text{C}/\text{Fe}] = 0$  (carbon abundance) and  $v_t = 2 \text{ km s}^{-1}$  (microturbulence) were assumed.

To keep consistency with our previous studies, the collisional rates ( $C_e$  for electron collisions and  $C_H$  for neutral hydrogen collisions) were computed by following the recipe described in subsection 3.1.3 of Takeda (1991). Namely, regarding electron collisions, we invoked Van Regemorter’s (1962) formula for permitted transitions ( $C_e^{(p)}$ ) and Auer and Mihalas’s (1973) equation (13) for forbidden transitions ( $C_e^{(f)}$ ). Meanwhile, as for hydrogen collision rates,  $C_H^{(p)}$  for permitted transition was evaluated by invoking Steenbock and Holweger’s (1984) formula, which is based on Drawin’s (1968, 1969) classical cross section, and  $C_H^{(f)}$  for forbidden transitions was approximated by simply scaling  $C_e^{(f)}$  according to the collision frequency (determined by the relative speed and the density of colliding particles) on the assumption of the same

<sup>2</sup> In addition, Altair (A7 V, rapid rotator with  $v_e \sin i \sim 200 \text{ km s}^{-1}$ ) was also observed to be used as a reference of telluric lines.

cross section. Since such computed  $C_{\text{H}} (= C_{\text{H}}^{(\text{p})} + C_{\text{H}}^{(\text{f})})$  has only order-of-magnitude accuracy at best and tends to be often overestimated, we also tested an alternative case of reduced  $C_{\text{H}}$  by introducing a reduction factor  $k$  as was done in Takeda and Honda (2005; cf. appendix 1 therein):

$$C_{\text{total}} = C_{\text{e}} + kC_{\text{H}}, \quad (1)$$

though we still assume  $k = 1$  as the standard case to be adopted. Such a scaling of  $C_{\text{H}}$  with  $k$  is applied also to bound-free collisional ionization rates, for which we invoked Jefferies (1968) for electron collisions and Steenbock and Holweger (1984) for neutral-hydrogen collisions.

We then interpolated Kurucz’s (1993) grid of ATLAS9 model atmospheres as well as the grid of the non-LTE departure coefficients in terms of  $T_{\text{eff}}$ ,  $\log g$ , and  $[\text{Fe}/\text{H}]$  to generate the atmospheric model and the departure coefficient data for each star.

Besides, for the reader’s convenience, extensive grids of non-LTE as well as LTE equivalent widths ( $EW^{\text{N}}$  and  $EW^{\text{L}}$ ) and non-LTE abundance corrections ( $\Delta$ ) for five multiplet 1 lines (C I 10683, 10685, 10691, 10707, 10729) were further computed for three  $[\text{C}/\text{Fe}]$  values ( $-0.3$ ,  $0.0$ , and  $+0.3$ ) and three  $v_{\text{t}}$  values (1, 2, and  $3 \text{ km s}^{-1}$ ), based on the non-LTE departure coefficients computed for 150 model atmospheres with two different treatments of neutral hydrogen collisions ( $k = 1$  and  $k = 0.1$ ), which are presented in electronic table E1.

### 3.2. Synthetic Spectrum Fitting

Inspecting the spectrum feature around  $\sim 1.07 \mu\text{m}$  (cf. figure 1), we decided to concentrate on the 10680–10697  $\text{\AA}$  region which comprises three C I lines (in which C I 10691 is the strongest one of multiplet 1) and two Si I lines. Then, following the similar way as in Papers I and II, we carried out non-LTE spectrum-synthesis analyses by applying Takeda’s (1995) automatic fitting procedure to this 17  $\text{\AA}$ -interval region while regarding the non-LTE carbon abundance ( $A_{\text{C}}^{\text{N}}$ ), LTE silicon abundance ( $A_{\text{Si}}^{\text{L}}$ ), the macrobroadening parameter ( $v_{\text{M}}$ ;  $e$ -folding half-width of the Gaussian macrobroadening function;  $\propto \exp[-(v/v_{\text{M}})^2]$ ), and the wavelength shift ( $\Delta\lambda$ ) as adjustable free parameters to be varied until a convergence is accomplished. The adopted atomic data of the relevant C I and Si I lines are presented in table 2. This fitting procedure turned out quite successful and  $A_{\text{C}}^{\text{N}}$  could be established for all 47 cases, though we had to fix the silicon abundance for two extremely metal-poor stars (BD +44 493 and G 64-37 [2009 July data]) where Si I lines are hardly visible. How the theoretical spectrum for the converged solutions fits well with the observed spectrum is displayed in figure 2 (2009 July data) as well as figure 3 (2011 August data). (Note that these two figures are arranged in analogy with figure 2 of Paper I and figure 1 of Paper II, respectively.) The resulting non-LTE C abundances ( $A_{\text{C}}^{\text{N}}$ ) are given in table 1, where the values of  $[\text{C}/\text{Fe}]$  ( $\equiv A_{\text{C}}^{\text{N}} - A_{\text{C}\odot}^{\text{N}} - [\text{Fe}/\text{H}]$ ; with  $A_{\text{C}\odot}^{\text{N}} = 8.54$  from Vesta) are also presented. More detailed results are found in electronic table E2, where the results of  $A_{\text{Si}}^{\text{L}}$  and  $v_{\text{M}}$  are also given.

### 3.3. Abundance-Related Quantities

While the non-LTE synthetic spectrum fitting directly yields the final abundance solution, this approach is not necessarily suitable when one wants to evaluate the extent of non-LTE corrections or to study the abundance sensitivity to changing the atmospheric parameters (i.e., it is tedious to repeat the fitting process again and again for different assumptions or different atmospheric parameters). Therefore, with the help of Kurucz’s (1993) WIDTH9 program (which had been considerably modified in various respects; e.g., inclusion of non-LTE effects, etc.), we computed the equivalent widths for each of the three C I lines ( $EW_{10683}$ ,  $EW_{10685}$ , and  $EW_{10691}$ ) “inversely” from the abundance solution (resulting from non-LTE spectrum synthesis) along with the adopted atmospheric model/parameters, since they are much easier to handle. Based on such evaluated  $EW$  values, the LTE abundances for each of the lines ( $A_{10683}^{\text{L}}$ ,  $A_{10685}^{\text{L}}$ , and  $A_{10691}^{\text{L}}$ ) were freshly computed, from which the non-LTE corrections ( $\Delta_{10683}$ ,  $\Delta_{10685}$ , and  $\Delta_{10691}$ ) were derived such as  $\Delta_{10683} \equiv A_{10683}^{\text{L}} - A_{\text{C}}^{\text{N}}$ , etc.

Besides, in order to examine the effect of changing  $C_{\text{H}}$  (neutral hydrogen collision rates), we also computed  $\Delta_{10691}$  ( $k = 0.1$ ) from  $EW_{10691}$  by using the non-LTE departure coefficients calculated for the  $k = 0.1$  case (i.e.,  $C_{\text{H}}$  is reduced by 1/10 from the adopted standard case of  $k = 1$ ) and evaluated the difference

$$\delta\Delta_{10691} \equiv \Delta_{10691}(k = 0.1) - \Delta_{10691}(k = 1). \quad (2)$$

We then estimated the uncertainties in  $A_{\text{C}}^{\text{N}}$  by repeating the analysis on  $EW_{10691}$  ( $EW$  for the strongest component) while perturbing the standard values of atmospheric parameters interchangeably by  $\pm 100 \text{ K}$  in  $T_{\text{eff}}$ ,  $\pm 0.2$  dex in  $\log g$ , and  $\pm 0.3 \text{ km s}^{-1}$  in  $v_{\text{t}}$  (which we regarded as typical uncertainties of the atmospheric parameters according to the original references; cf. subsection 4.2 in Paper I). Let us call these six kinds of abundance variations as  $\delta_{T+}$ ,  $\delta_{T-}$ ,  $\delta_{g+}$ ,  $\delta_{g-}$ ,  $\delta_{v+}$ , and  $\delta_{v-}$ , respectively. We then computed the root-sum-square of three quantities  $\delta_{Tgv} \equiv (\delta_{T+}^2 + \delta_{g+}^2 + \delta_{v+}^2)^{1/2}$  as the abundance uncertainty (due to combined errors in  $T_{\text{eff}}$ ,  $\log g$ , and  $v_{\text{t}}$ ), where  $\delta_{T+}$ ,  $\delta_{g+}$ , and  $\delta_{v+}$  are defined as  $\delta_{T+} \equiv (|\delta_{T+}| + |\delta_{T-}|)/2$ ,  $\delta_{g+} \equiv (|\delta_{g+}| + |\delta_{g-}|)/2$ , and  $\delta_{v+} \equiv (|\delta_{v+}| + |\delta_{v-}|)/2$ , respectively.

The resulting  $[\text{C}/\text{Fe}]$ ,  $\Delta_{10691}$ ,  $\delta\Delta_{10691}$ , and  $EW_{10691}$  for each star are plotted against  $T_{\text{eff}}$  in figures 4 a–d, where  $\log g > 3.0$  stars (dwarfs) and  $\log g < 3.0$  stars (giants) are distinguished by filled and open symbols, respectively, and the error bar attached to  $[\text{C}/\text{Fe}]$  represents  $\pm\delta_{Tgv}$ . While only  $A_{\text{C}}^{\text{N}}$ ,  $EW_{10691}$ ,  $\Delta_{10691}$ , and  $[\text{C}/\text{Fe}]$  are given in table 1, all the relevant data (including  $EW$  and  $\Delta$  for all three lines and each of the  $\delta$  values) are presented in electronic table E2.

It can be seen from figure 4a that the typical extent of  $\delta_{Tgv}$  is  $\lesssim 0.1$ – $0.2$  dex and not very significant. We should bear in mind, however, that the non-LTE corrections are so large and that some uncertainties in them are more or less inevitable. Apart from the ambiguities in

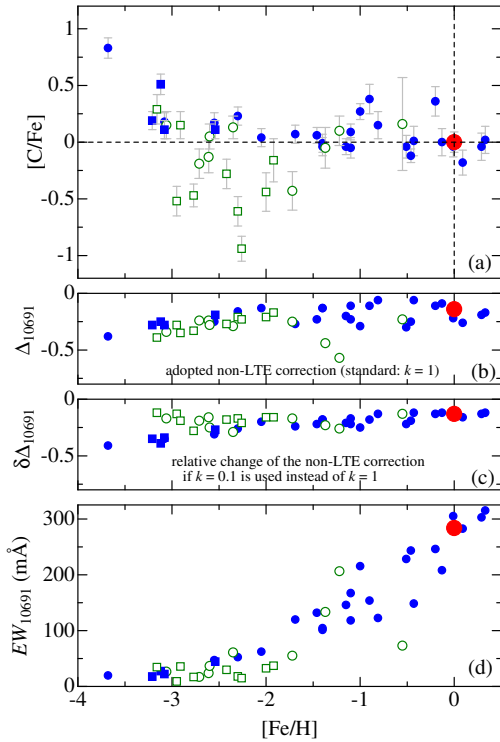


**Fig. 4.** Carbon abundances (along with the related quantities) plotted against  $[\text{Fe}/\text{H}]$ : (a)  $[\text{C}/\text{Fe}]$  (C-to-Fe logarithmic abundance ratio corresponding to non-LTE carbon abundance; where attached error bars represent the ambiguities due to uncertainties in the atmospheric parameters ( $\delta T_{\text{eff}}$ ; cf. subsection 3.3) (b)  $\Delta_{10691}$  (non-LTE correction for the C I 10691 line derived with the standard classical treatment of neutral-hydrogen collisions with  $k = 1$ ). (c)  $\delta\Delta_{10691}$  (relative difference of non-LTE correction caused by reducing the neutral-hydrogen collisions by 1/10; cf. equation (2)). (d)  $EW_{10691}$  (equivalent width for the C I 10691 line). Dwarfs ( $\log g > 3$ ) and giants ( $\log g < 3$ ) are discriminated by filled (blue) and open (green) symbols, respectively. The results for 33 stars based on the 2009 July data and those for 12 stars based on the 2011 August data are shown by circles and squares, respectively. The large red filled circle denotes the Sun (Vesta).

the treatment of collisional rates due to neutral hydrogen collisions (choice of  $k$ ) as discussed later in subsections 4.1 and 4.3, we should recall that our non-LTE calculations were done on the condition of  $[\text{C}/\text{Fe}] = 0$ . Actually, this assumption is reasonable, since most of the  $[\text{C}/\text{Fe}]$  values derived for our targets scatter around  $\sim 0$  with a dispersion of  $\sim \pm 0.5$  dex (figure 4a). However,  $[\text{C}/\text{Fe}]$  values of two stars considerably depart from zero; i.e.,  $+0.83$  (BD +44 493) and  $-0.94$  (HD 13979), for which the mismatch of  $[\text{C}/\text{Fe}]$  may cause some errors. As a test, we evaluated the abundance change when we used departure coefficients computed with  $[\text{C}/\text{Fe}] = +1.0$  (BD +44 493) and  $[\text{C}/\text{Fe}] = -1.0$  (HD 13979) instead of  $[\text{C}/\text{Fe}] = 0$ . These calculations were done on the selected two models (t55g40m40 and t50g20m20 included in the model grid of electronic table E1) having parameters closest to those of these two stars. We then found that the extent of

non-LTE overpopulation for the relevant high-excitation term is enhanced/reduced by decreasing/increasing the C abundance,<sup>3</sup> and thus the  $A_{\text{C}}^{\text{N}}$  (derived for the same  $EW$ ) is increased by 0.25 dex ( $[\text{C}/\text{Fe}] = +1.0$ ; BD +44 493) and reduced by 0.10 dex ( $[\text{C}/\text{Fe}] = -1.0$ ; HD 13979) compared to the results for the standard  $[\text{C}/\text{Fe}] = 0.0$  case. Accordingly, the error caused by applying the departure coefficients computed with  $[\text{C}/\text{Fe}] = 0$  to such exceptional cases of considerably peculiar C abundance would be  $\sim 0.1$ – $0.2$  dex.

## 4. Discussion

### 4.1. Line Strength and Non-LTE Effect

According to figures 4b–d and table 1, the following features are recognized regarding the behavior of the strength and the non-LTE correction of the C I 10691 line (the strongest among the multiplet 1 lines at  $\lambda 1.07 \mu\text{m}$ ).

— The C I 10691 line is clearly visible even for extremely metal-poor stars ( $[\text{Fe}/\text{H}] \lesssim -3$ ) with  $EW$  on the order of  $\sim 10 \text{ m}\text{\AA}$ , irrespective of dwarfs or giants, which suggests the usability of this line to explore the carbon synthesis history of the Galaxy.

— The non-LTE correction is always negative (corresponding to non-LTE line-strengthening). While the typical extent of  $|\Delta_{10691}|$  for the standard  $k = 1$  case is several tenths dex ( $\lesssim 0.5$  dex; cf. figure 4b), it is further raised by almost a similar amount when  $k$  is reduced from 1 to 0.1 (figure 4d) which makes  $|\Delta_{10691}(k = 0.1)|$  even up to  $\lesssim 1$  dex. This implies that the non-LTE correction is sensitive to how the neutral hydrogen collision is treated.<sup>4</sup>

— The extent of  $|\Delta_{10691}|$  systematically increases with a decrease in  $[\text{Fe}/\text{H}]$ , despite that the line strength is weakened, which means that the non-LTE correction becomes progressively more important as we go toward the extremely metal-poor regime.

In order to help our understanding of these features mentioned above, we display in figure 5 how  $EW^{\text{N}}$  (theoretical non-LTE equivalent width computed for the C I

<sup>3</sup> This trend could be interpreted as due to the efficiency change in the UV pumping from ground or low-excitation levels to upper levels of high excitation, which may possibly depend upon the C abundance in the very metal-poor regime. That is, as long as such UV transitions are optically thick and in radiative detailed balance, such process does not occur. Meanwhile, as the C abundance is sufficiently lowered and some of these UV transitions eventually become optically thin, high-excitation C I levels may get overpopulated via upward pumping by absorbing hot UV continuum radiation.

<sup>4</sup> This does not agree with the conclusion of Fabbian et al. (2006, 2009), who found that the non-LTE corrections for C I lines are insensitive to a choice of the reduction factor ( $S_{\text{H}}$  in their notation); even changing  $S_{\text{H}} = 1$  to  $S_{\text{H}} = 0$  makes only an insignificant change ( $\sim 0.1$  dex) in their non-LTE corrections for C I 9061–9111 lines of multiplet 3, which are as large as those of C I 10683–10691 lines of multiplet 1 (cf. figure 8b). Considering the more or less reasonable consistency between the  $\Delta$  (multiplet 3) values of Takeda and Honda (2005) (see also the Appendix of this paper) and those of Fabbian et al. (2006; cf. their figure 8), this discrepancy is hard to understand. Although the cause is not clear, something may be different between their and our calculation procedures.

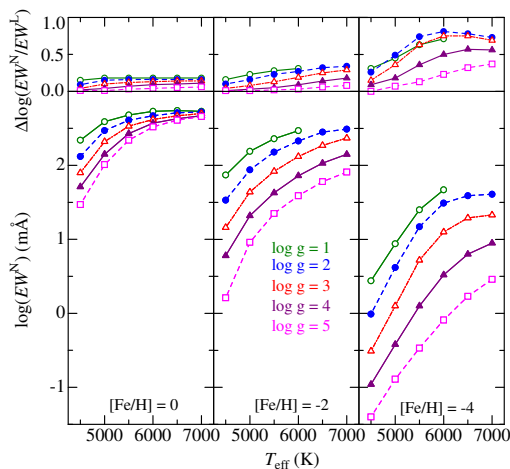


**Fig. 5.** Theoretically computed non-LTE logarithmic equivalent widths ( $\log EW^N$ ; lower panels) and the difference between non-LTE and LTE logarithmic equivalent widths ( $\log EW^N - \log EW^L$ ; upper panels) plotted against  $T_{\text{eff}}$ , which were calculated for the C I 10691.24 line with the standard treatment of H I collision cross sections ( $k = 1$ ),  $v_t = 2 \text{ km s}^{-1}$ , and  $[\text{C}/\text{Fe}] = 0$ . The left, middle, and right panels correspond to  $[\text{Fe}/\text{H}] = 0, -2$ , and  $-4$ , respectively. Open circles, filled circles, open triangles, filled triangles, and open squares denote results for  $\log g = 1, 2, 3, 4$ , and  $5$ , respectively.

10691 line) and  $EW^N/EW^L$  (non-LTE to LTE equivalent-width ratio) depend on  $T_{\text{eff}}$ ,  $\log g$ , and  $[\text{Fe}/\text{H}]$ , based on the data in electronic table E1 (cf. subsection 3.1) corresponding to the standard  $k = 1$  case. We can learn from this figure significant characteristics concerning the line-strength behaviors:

— While it is natural that the line is weakened with a decrease in  $[\text{Fe}/\text{H}]$  ( $=[\text{C}/\text{H}]$ ), its strength grows with an increase in  $T_{\text{eff}}$  as well as with a decrease in  $\log g$ .

— The non-LTE to LTE strength ratio is always larger than unity (i.e., non-LTE line strengthening) as we already recognized from the negative sign of  $\Delta$ , which increases with a lowering of the metallicity; it amounts up to  $\gtrsim 5$  at  $[\text{Fe}/\text{H}] = -4$ , which explains the  $[\text{Fe}/\text{H}]$ -dependence of  $|\Delta|$  mentioned above.

— We may interpret these trends in terms of the ionization degree of carbon (partially ionized in the atmospheres of FGK stars), which tends to enhance with an increase in  $T_{\text{eff}}$  as well as with a decrease in  $\log g$  (lowered density) and  $[\text{Fe}/\text{H}]$  (lowered electron density, enhanced UV overionizing radiation due to the increased transparency), while the change in the  $\text{H}^-$  continuum opacity is also involved especially in the  $\log g$ -effect. That is, the population of high-excitation C I lines is closely coupled with the population of C II parent term (i.e., the effect of  $n^{(\text{II})}/n^{(\text{I})\dagger}$ ; cf. section 3 in Takeda 1992), which makes the population of high-excitation C I level larger as the ionization fraction (C II/C I) increases. Therefore, the degree of ionization plays an important role in understanding the strengths and the non-LTE effect of high-excited C I lines such as those of multiplet 1 or 3.

— Besides, under the considerably metal-poor condition

of very low C abundance, some of the strong C I transitions in UV would become optically thin, which may act to enhance non-LTE overpopulation of high-excitation levels via the pumping effect (cf. footnote 3).

— Thus, the mechanism of non-LTE line intensification is not necessarily the same for the strong-line case of near-solar metallicity and the weak-line case of very low metallicity. In the former situation, the line is strengthened significantly by the dilution of the line source function due to photon escape (such as the case of a simple two-level atom), while the increase of line-opacity due to overpopulation in the lower level of this transition is essential for the latter case.

#### 4.2. Comparison with Literature Data

We now discuss the carbon abundances we have derived in comparison with previous studies taken from the literature.

According to figure 4a, our  $[\text{C}/\text{Fe}]$  vs.  $[\text{Fe}/\text{H}]$  relation constructed from 47 objects is characterized by (i) a gradual increase of  $[\text{C}/\text{Fe}]$  at a slightly supersolar level with a decrease of  $[\text{Fe}/\text{H}]$  from  $\sim 0$  to  $\sim -1$ , (ii) a subsolar  $[\text{C}/\text{Fe}]$  around  $\sim -0.5$  (mostly giants) at  $-3 \lesssim [\text{Fe}/\text{H}] \lesssim -2$ , and (iii) upturn of  $[\text{C}/\text{Fe}]$  toward appearance of supersolar  $[\text{C}/\text{Fe}]$  at the extremely metal-poor regime ( $-4 \lesssim [\text{Fe}/\text{H}] \lesssim -3$ ). Actually, these features are in good agreement with what has been established so far; e.g., figure 6 of Norris, Ryan, and Beers (1997) is quite similar to our figure 4a. Accordingly, we may state that our analysis using C I 10683/10685/10691 lines has yielded  $[\text{C}/\text{Fe}]$  results consistent with other previous work (where CH lines were mainly used in the very metal-poor regime) at least in the qualitative sense.

We then turn to the comparison of our  $[\text{C}/\text{H}]$  ( $\equiv A_{\text{C}}^{\text{N}} - A_{\text{C}\odot}^{\text{N}}$ ) for individual stars with the literature data summarized in table 3, which we collected mainly by invoking the SAGA database (cf. section 1) and by adding data from several papers by ourselves (see the caption of table 3). We could thus get the published data for 37 stars ( $\sim 80\%$  of the total objects). These literature  $[\text{C}/\text{H}]$  values are plotted by crosses (red  $\cdots$  molecular lines mostly of CH, blue  $\cdots$  C I lines) in figure 6, where our results are designated by circles (open  $\cdots$  giants, filled  $\cdots$  dwarfs). Several notable characteristics can be read from this figure:

— For disk stars with metallicity of  $-1 \lesssim [\text{Fe}/\text{H}]$  where C I lines are mostly used, the agreement is generally good, without any systematic discrepancy.

— In contrast, at the very low metallicity range ( $-2.7 \lesssim [\text{Fe}/\text{H}] \lesssim -1$ ), we note that literature  $[\text{C}/\text{H}]$  values derived from CH lines (red crosses) tend to be appreciably lower (typically by several tenths dex) than our results, especially for low-gravity giants (open circles).<sup>5</sup> Meanwhile,

<sup>5</sup> Actually, such a CH vs. C I discrepancy is apparently observed in the results of Tomkin et al. (1992), which is a rare study because two kinds of C abundances from C I lines and CH molecular band are given for a star. According to their table 4, the average difference for 28 stars (in which both abundances are available) is  $\langle A(\text{CH}) - A(\text{C I}) \rangle = -0.41$  dex, which is nearly on the same order as we see in figure 6. We should note, how-

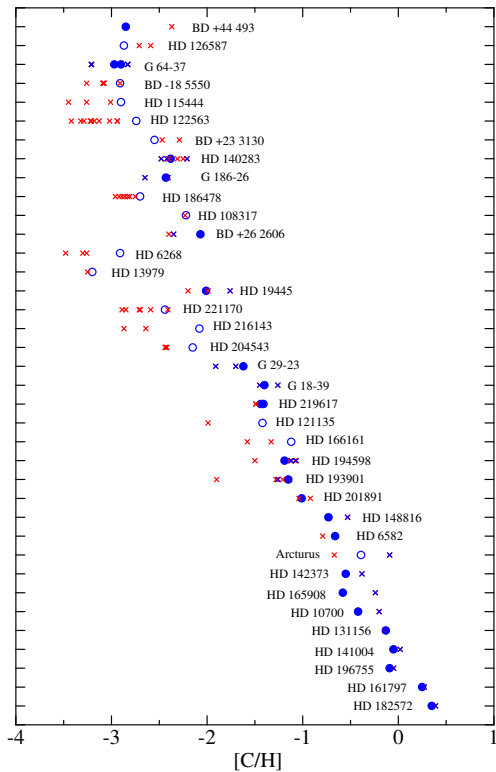


**Fig. 6.** Comparison of  $[C/H]$  ( $\equiv A_C - A_{C\odot}$ ) values derived in this study (circles, where open and filled symbols denote giants and dwarfs, respectively) with those taken from various published studies (crosses, where those derived from molecular and atomic lines are discriminated in red and blue colors, respectively), based on the data summarized in table 3. Stars are arranged in the ascending order of  $[Fe/H]$  from top to bottom.

those derived from C I lines (mostly 9061–9111 lines of multiplet 3) expressed by blue crosses do not show such a systematic tendency.

— However, if we confine to extremely metal-poor stars at  $[Fe/H] \lesssim -3$ , such a trend can not be clearly seen; e.g., CH-based literature  $[C/H]$ 's are even higher than our results in HD 126587 and BD +44 493.

— Roughly summarizing, we may state that our C-abundances determined from C I 10683–10691 lines are almost consistent with the literature results if they are based on C I lines, while CH-based abundances published so far tend to be lower than ours (especially for giants).

#### 4.3. Merits and Problems of C I $1.07\mu\text{m}$ Lines

Returning to the motivation of this study described in section 1, we again question to ourselves: Are C I  $1.07\mu\text{m}$  lines of multiplet 1 practically useful for stellar carbon abundance determinations, especially for very metal-poor

ever, that the real discordance could be much more serious (even amounting up to  $\gtrsim 1$  dex), since  $A(\text{CH})$  may further be significantly lowered (e.g., by a few tenths dex to  $\lesssim 1$  dex; especially at the very metal-poor condition) when new 3D model atmospheres are used (e.g., Asplund 2005; Collet 2007) because of the reduced temperature at the upper layers.

stars? Our answer is as follows: “Yes, definitely. We believe that these near-IR lines would promisingly be applied to investigate C abundances for a variety of stars. However, several things still remain to be done before we can assure a sufficient precision in abundance determinations.”

We summarize below the favorable characteristic of these C I lines in comparison to other indicators.

— These C I lines have sufficiently large strengths and would be visible down to extremely low-metallicity region. According to figure 5, if we could measure a very weak line of  $EW \lesssim 10$  mÅ based on a high dispersion (e.g.,  $R \sim 30000$ – $50000$ ) and high S/N (e.g.,  $\sim 300$ – $500$ ) spectrum,  $A_C$  of a  $[Fe/H] \sim -4$  star would be determinable even for the case of  $[C/Fe] \sim 0$  (of course, detection becomes much easier for carbon-enhanced stars of  $[C/Fe] > 0$ ).

— This merit almost equally applies to stars of any type, since whether a star is a giant or a dwarf does not significantly affect the line strength. That is, since dwarfs with higher  $\log g$  tend to have higher  $T_{\text{eff}}$  (e.g., turn-off stars with  $T_{\text{eff}} \sim 6000$  K and  $\log g \sim 4$ ) and giants with lower  $\log g$  tend to have lower  $T_{\text{eff}}$  (e.g., evolved red giants with  $T_{\text{eff}} \sim 4000$  K and  $\log g \sim 1$ ) as shown in figure 1a of Paper I, these two opposite effect of  $T_{\text{eff}}$  and  $\log g$  tend to cancel with each other (cf. figure 5), which makes the line strength rather insensitive to  $T_{\text{eff}}$  as well as  $\log g$ .

— Carbon abundances from CH molecular lines are very sensitive to  $T_{\text{eff}}$  (cf. table 5 of Tomkin et al. 1992), as well as to the temperature structure in the upper layer and to the 3D effect (e.g., Asplund 2005; Behara et al. 2008). In this respect, C I lines are much less sensitive to such effects.

— These C I 10683–10691 lines of multiplet 1 are more advantageous than the C I 9061–9111 lines of multiplet 3, because they are stronger and situate in a spectral region almost free from telluric lines.

Despite these merits, however, we have to keep in mind that problems still remain in deriving the C abundances from these C I lines, especially when a sufficient precision is pursued. Above all, given that these lines are subject to rather a large non-LTE effect, attention should be paid to use as reliable non-LTE abundance corrections as possible. Here, the difficult problem is the treatment of collisions with neutral hydrogen atoms, or how to choose the value of  $k$  in equation (1). Since the non-LTE corrections appreciably depend upon this parameter (as we can see from figure 4c), its adequate choice is mandatory.

Yet, we consider that  $k = 1$  adopted in this investigation (as in our past studies) is reasonable for the following reasons:

— If we use  $k = 0.1$ , for example, we would obtain  $A_{C,\odot}^N = 8.40$  ( $\Delta = -0.28$ ) as the solar carbon abundance (instead of 8.54 for  $k = 1$ ). Although this value is almost the same as the most recent solar C abundance of 8.43 claimed by Asplund et al. (2009) using the state-of-the-art 3D model, our result based on the classical 1D model should not be directly compared to it. Considering that Takeda and Honda (2005) derived the solar C abundances

of 8.49, 8.76, and 8.70 (based on the same solar model as used in this study) from three non-LTE insensitive lines ([C I] 8727, C I 5052, and C I 5380), we feel reluctant to further lower the value of 8.54.

— Admittedly, the problematic discrepancy between our [C/H] results and those from CH molecular lines seen in metal-poor giants (cf. subsection 4.2) may significantly be mitigated by reducing  $k$ . If we do so, however, our C I-based abundances for dwarfs would be overcorrected (actually, non-LTE corrections for dwarfs are more sensitive to  $k$  than those of giants; cf. figure 4d) to become discordant with the literature results, since the consistency between CH and C I results are not so bad in metal-poor dwarfs unlike the case for giants (cf. figure 6). We rather suspect that CH-based abundances of giants may have been incorrect. Given that modeling of giants atmosphere is generally less reliable than the case of dwarfs, previously published C abundances of metal-poor giants based on CH lines may have been appreciably underestimated due to some imperfectness of the atmospheric model, reflecting the enormous sensitivity of molecular lines to errors in the temperature structure. For example, since the ubiquitous existence of chromospheric activities even in very metal-poor old stars is evidenced by the detection of He I 10830 line (cf. Takeda & Takada-Hidai 2011b), the temperature of molecule-forming upper layers may be higher than that predicted by classical model atmospheres or UV radiation coming from the chromosphere may promote non-thermal dissociation of molecules in the photosphere, which would lead to underestimation of carbon abundances derived from CH molecular band (if based on the conventional method of analysis).

In any event, it is very important to determine the value of  $k$  in an empirical manner. One way for doing this may be to require the abundance consistency between different lines, such as done by Takeda and Honda (2005, cf. appendix 1 therein) for oxygen lines. Actually we challenged it by comparing the abundances from lines of multiplet 1 and multiplet 3, as described in the Appendix. Unfortunately, this trial turned out unsuccessful, because the  $k$ -sensitivity of these two line groups were essentially the same. As an alternative approach, it would be promising to compare the center-to-limb variation of C I 10683–10691 lines on the solar disk with the simulations done for various  $k$  values, as recently tried by Pereira, Kiselman, and Asplund (2009a) as well as Pereira, Asplund, and Kiselman (2009b) for the oxygen lines. We would be able to use these near-IR C I lines for precise C abundance determinations with confidence, when the calibration of this collisional parameter has been established.

## 5. Conclusion

Motivated by the fact that C I lines at  $\sim 1.07 \mu\text{m}$  (multiplet 1) have barely been exploited for stellar C abundance studies so far, despite their sufficient strengths and being in a favorable spectral region free from telluric lines, we carried out a non-LTE spectrum-fitting analysis of C I 10683–10691 lines for selected 46 halo/disk stars in a wide

metallicity range ( $\sim -3.7 [\text{Fe}/\text{H}] \lesssim +0.3$ ) based on the  $zJ$ -band spectral data collected with IRCS+AO188 of the Subaru Telescope, with an aim of examining whether the C abundances can be successfully determined by these lines especially for very metal-poor stars where lines of CH molecules have been mainly invoked.

These C I lines were confirmed to be clearly visible, from which C abundances could be successfully determined for all stars down to  $[\text{Fe}/\text{H}] \sim -3.7$ . The resulting [C/Fe] vs. [Fe/H] diagram revealed the well-known trend established by previous studies; such as a gradual increase of [C/Fe] with a decrease of [Fe/H] from  $\sim 0$  to  $\sim -1$ , subsolar [C/Fe] of  $\sim -0.5$  at  $-3 \lesssim [\text{Fe}/\text{H}] \lesssim -2$ , and upturn of [C/Fe] toward appearance of supersolar [C/Fe] at  $-4 \lesssim [\text{Fe}/\text{H}] \lesssim -3$ . We may thus regard that our analysis is consistent with previous studies at least qualitatively.

We also compared the resulting [C/H] for individual stars with the published data collected from various literature (data for 37 stars were available). While the agreement is mostly good for disk stars ( $-1 \lesssim [\text{Fe}/\text{H}]$ ) where C I lines are generally used, we found that the literature [C/H] values of very metal-poor stars ( $-2.7 \lesssim [\text{Fe}/\text{H}] \lesssim -1$ ) derived from CH lines tend to be appreciably lower than our results especially for low-gravity giants, though those derived from C I 9061–9111 lines of multiplet 3 do not show such a systematic tendency. The reason for this disagreement is yet to be investigated.

Since the abundances of these neutral C lines are subject to an appreciably large non-LTE effect (typically by several tenths dex) whose importance progressively grows as the metallicity is lowered, attention should be paid to the reliability of non-LTE corrections to be applied. Here, the difficult problem is how to treat collisions with neutral hydrogen atoms, for which classical rates are often multiplied by a reduction factor  $k (\leq 1)$ . Although we consider that the choice of  $k = 1$  (standard classical treatment) is still reasonable, its choice has a significant influence on the extent of non-LTE effect (e.g., if we use  $k = 0.1$ , non-LTE corrections would become twice as large as the  $k = 1$  case). Thus, establishing  $k$  in some empirical manner (e.g., by using the center-to-disk variation on the solar disk) is urgently awaited.

One of the authors (M. T.-H.) is grateful for a financial support from a grant-in-aid for scientific research (C, No. 22540255) from the Japan Society for the Promotion of Science.

This research has made extensive use of the SAGA database system, maintained by Takuma Suda, Yutaka Katsuta, and Shimako Yamada.

## Appendix. Non-LTE Corrections of C I 9061–9111 Lines Revisited

Takeda and Honda (2005; cf. appendix 2 therein) computed an extensive grid of non-LTE equivalent widths and abundance corrections for five C I lines of multiplet 3 ( $3s^3P^o - 3p^3P$ ) at 9061.44, 9078.29, 9088.51, 9094.83, and 9111.81  $\text{\AA}$ . They also carried out a non-LTE reanalysis of

published equivalent-width data of these C I 9061–9111 lines along with those of C I 7111–7119 lines (multiplet 26, 25.02).

Having reexamined those previous calculations, we realized that there was a mis-assignment of departure coefficients in computing the non-LTE equivalent widths of C I 9061–9111 lines. More precisely, we had erroneously used the departure coefficients corresponding to multiplet 1 ( $3s\ ^3P^o - 3p\ ^3D$ ) for these multiplet 3 lines. Accordingly, we decided to redo the calculations (this time, computations were performed not only for  $k = 1$  as assumed before, but also for  $k = 0.1$ ), and the resulting grids of new non-LTE corrections ( $\Delta$ ) and equivalent-widths ( $EW$ ) are presented in electronic table E1 along with those of C I 10685–10729 lines.

Comparing the new results with the old ones, we realized that the differences are insignificant; actually, the change of  $\Delta$  is  $\lesssim 0.1$  dex at most, as shown in figure 7. This is due to the fortunate fact that multiplets 1 and 3 have the same lower term ( $3s\ ^3P^o$ ), while the upper terms ( $3p\ ^3D$  and  $3p\ ^3P$ ) have similar departure coefficients because they lie closely to each other. Accordingly, we do not see any need to apply significant changes to what is described in appendix 2 of Takeda and Honda (2005), which still remain essentially valid in the practical sense.

In connection with the newly recomputed non-LTE corrections for multiplet 3 lines, we tried to empirically determine the value of  $k$  defined in equation (1) by requiring the consistency between the carbon abundances derived from C I 10685–10691 lines (obtained from this study) and those from C I 9061–9111 lines (based on re-analysis of published equivalent widths). By consulting the work of Akerman et al. (2004),  $EW$ s of 9061–9111 lines for 8 stars were available, from which we derived the mean abundance of each star for three choices of  $k$ :  $k = 0.1$ ,  $k = 1$ , and  $k = \infty$  (i.e., LTE). Comparison of such computed  $A_C(9061\text{--}9111\text{:RMT 3})$  with our  $A_C(10685\text{--}10691\text{:RMT 1})$  is presented in figure 8a. Unfortunately, we can recognize from this figure that the  $k$ -sensitivity of both multiplet lines is nearly the same with each other, which means that empirically establishing  $k$  by the requirement of  $A_C(\text{RMT 1}) = A_C(\text{RMT 3})$  is hardly practicable (cf. figure 8b). We would have to find some other different carbon lines to be compared, in order to accomplish this aim.

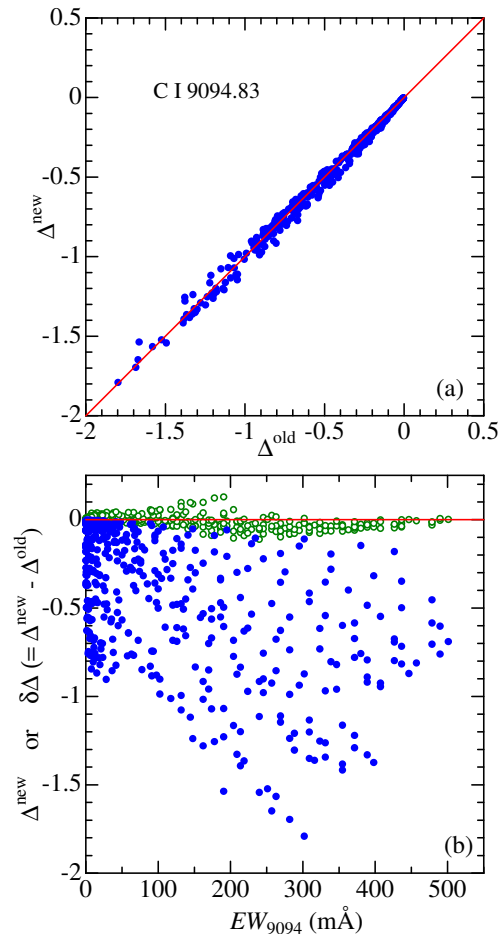


**Fig. 7.** (a) Comparison of the old non-LTE corrections ( $\Delta^{\text{old}}$ ) for the 9094.83 line (the strongest one of the five 9061–9111 lines of RMT 3) computed by Takeda and Honda (2005; cf. appendix 2 therein) for an extensive grid of model atmospheres, for which we found that departure coefficients for the upper term had been erroneously assigned by mistake, with the new results ( $\Delta^{\text{new}}$ ) correctly recomputed in this study. Note that these calculations correspond to  $k = 1$  (standard treatment of neutral hydrogen collisions). (b) Similarly to panel (a),  $\Delta^{\text{new}}$  (filled symbols) and the difference  $\delta\Delta$  ( $\equiv \Delta^{\text{new}} - \Delta^{\text{old}}$ ; open symbols) are plotted against the (non-LTE) equivalent width ( $EW_{9094}$ ).



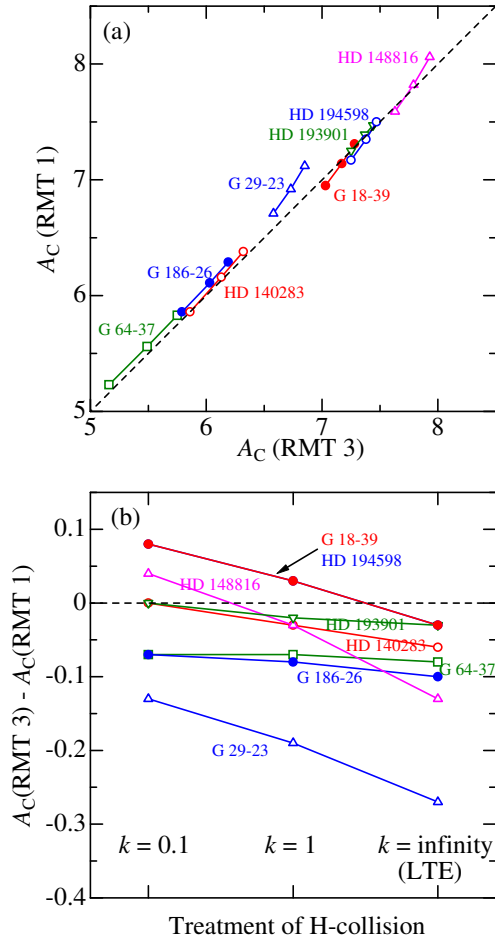


**Fig. 8.** (a) Comparison of the carbon abundances ( $A_C$ ) of 8 stars derived from this study (C I 10683–10691 lines of RMT 1) with those obtained by reanalyzing Akerman et al.'s (2004) *EW* data of C I 9061–9111 lines (RMT 3), where three different conditions were adopted regarding how neutral hydrogen collisions ( $C_H$ ) are taken into account: (i) LTE ( $k = \infty$ ), (ii) standard treatment ( $k = 1$ ), and (iii) reduction of  $C_H$  by 1/10 ( $k = 0.1$ ); note that  $A_C(\text{i}) > A_C(\text{ii}) > A_C(\text{iii})$  generally holds. (b) Graphical display of how  $A_C(\text{RMT 3}) - A_C(\text{RMT 1})$  varies with a different choice in the treatment of  $C_H$ .

## References

- Akerman, C. J., Carigi, L., Nissen, P. E., Pettini, M., & Asplund, M. 2004, *A&A*, 414, 931
- Aoki, W., et al. 2002, *PASJ*, 54, 427
- Aoki, W., et al. 2005, *ApJ*, 632, 611
- Aoki, W., et al. 2007, *ApJ*, 660, 747
- Aoki, W., & Honda, S. 2008, *PASJ*, 60, L7
- Asplund, M. 2005, *ARA&A*, 43, 481
- Asplund, M., Grevesse, N., Sauval, A. J., & Scott, P. 2009, *ARA&A*, 47, 481
- Auer, L. H., & Mihalas, D. 1973, *ApJ*, 184, 151
- Barklem, P.S., et al. 2005, *A&A*, 439, 129
- Behara, N., Bonifacio, P., Ludwig, H. G., Sbordone, L., Gonzalez Hernandez, J. I., & Caffau, E. 2008, in *Proc. 10th Symposium on Nuclei in the Cosmos*<sup>6</sup>
- Cayrel, R., et al. 2004, *A&A*, 416, 1117
- Collet, R., Asplund, M., & Trampedach, R. 2007, *A&A*, 469, 687
- Drawin, H. W. 1968, *Z. Physik*, 211, 404
- Drawin, H. W. 1969, *Z. Physik*, 225, 483
- Fabbian, D., Asplund, M., Carlsson, M., & Kiselman, D. 2006, *A&A*, 458, 899
- Fabbian, D., Nissen, P. E., Asplund, M., Pettini, M., & Akerman, C. 2009, *A&A*, 500, 1143
- Gratton, R. G., Sneden, C., Carretta, E., & Bragaglia, A. 2000, *A&A*, 354, 169
- Grevesse, N., Noels, A., & Sauval, A. J. 1996, *ASP Conf. Ser.* 99, 117
- Honda, S., Aoki, W., Kajino, T., Ando, H., Beers, T., Izumiura, H., Sadakane, K., & Takada-Hidai, M. 2004, *ApJ*, 607, 474
- Ito, H., Aoki, W., Honda, S., & Beers, T. C. 2009, *ApJ*, 698, L37
- Ivans, I. I., Simmerer, J., Sneden, J., Lawler, J. E., Cowan, J. J., Galino, R., & Bisterzo, S. 2006, *ApJ*, 645, 613
- Jefferies, J. T. 1968, *Spectral Line Formation* (Waltham: Blaisdel)
- Johnson, J. A., Herwig, F., Beers, T. C., & Christlieb, N. 2007, *ApJ*, 658, 1203
- Kjærgaard, P., Gustafsson, B., Walker, G. A. H., & Hultqvist, L. 1982, *A&A*, 115, 145
- Kurucz, R. L. 1993, *Kurucz CD-ROM, No. 13, ATLAS9 Stellar Atmosphere Program and 2 km/s Grid* (Cambridge, MA: Harvard-Smithsonian Center for Astrophysics)<sup>7</sup>
- Kurucz, R. L., & Bell, B. 1995, *Kurucz CD-ROM, No. 23, Atomic Line Data* (Cambridge, MA: Harvard-Smithsonian Center for Astrophysics)<sup>8</sup>
- Lai, D. K., Johnson, J. A., Bolte, M., & Lucatello, S. 2007, *ApJ*, 667, 1185
- Lai, D. K., Bolte, M., Johnson, J. A., & Lucatello, S., Heger, A., & Woosley, S. E. 2008, *ApJ*, 681, 1524
- Leushin, V. V., & Topil'skaya, G. P. 1986, *Astrophysics*, 25, 415
- McWilliam, A., Preston, G. W., Sneden, C., & Searle, L. 1995, *AJ*, 109, 2757
- Meléndez, J., & Barbuy, B. 2002, *ApJ*, 575, 474
- Meléndez, J., Barbuy, B., & Spite, F. 2001, *ApJ*, 556, 858

<sup>6</sup> Available at <http://pos.sissa.it/cgi-bin/reader/conf.cgi?confid=53>

<sup>7</sup> Available at <http://kurucz.harvard.edu/PROGRAMS.html>.

<sup>8</sup> Available at <http://kurucz.harvard.edu/LINELISTS.html>.

- Moore, C. E. 1959, A Multiplet Table of Astrophysical Interest; NBS Technical Note No. 36, Reprinted Version of 1945 edition (Washington DC: US Department of Commerce)
- Norris, J. E., Ryan, S. G., & Beers, T. C. 1997, *ApJ*, 488, 350
- Pereira, T. M. D., Kiselman, D., & Asplund, M. 2009, *A&A*, 507, 417
- Pereira, T. M. D., Asplund, M., & Kiselman, D. 2009, *A&A*, 508, 1403
- Ramírez, I., & Allende Prieto, C. 2011, *ApJ*, 743, 135
- Simmerer, J., Sneden, C., Cowan, J. J., Collier, J., Woolf, V. M., & Lawler, J. E. 2004, *ApJ*, 617, 1091
- Spite, M., et al. 2005, *A&A*, 430, 655
- Spite, M., et al. 2006, *A&A*, 455, 291
- Steenbock, W., & Holweger, H. 1984, *A&A*, 130, 319
- Stürenburg, S., & Holweger, H. 1990, *A&A*, 237, 125 [Erratum in *A&A*, 246, 644]
- Suda, T., et al. 2008, *PASJ*, 60, 1159
- Suda, T., Yamada, S., Katsuta, Y., Komiya, Y., Ishizuka, C., Aoki, W., & Fujimoto, M. Y. 2011, *MNRAS*, 412, 843
- Takeda, Y. 1991, *A&A*, 242, 455
- Takeda, Y. 1992, *PASJ*, 44, 649
- Takeda, Y. 1994, *PASJ*, 46, 53
- Takeda, Y. 1995, *PASJ*, 47, 287
- Takeda, Y., & Honda, S. 2005, *PASJ*, 57, 65
- Takeda, Y., & Takada-Hidai, M. 2011a, *PASJ*, 63, S537 (Paper I)
- Takeda, Y., & Takada-Hidai, M. 2011b, *PASJ*, 63, S547
- Takeda, Y., & Takada-Hidai, M. 2012, *PASJ*, 64, 42 (Paper II)
- Tomkin, J., Lemke, M., Lambert, D., & Sneden, C. 1992, *AJ*, 104, 1568
- Van Regemorter, H. 1962, *ApJ*, 136, 906
- Zhang, L., Karlsson, T., Christlieb, N., Korn, A. J., Barklem, P.S., & Zhao, G. 2011, *A&A*, 528, A92

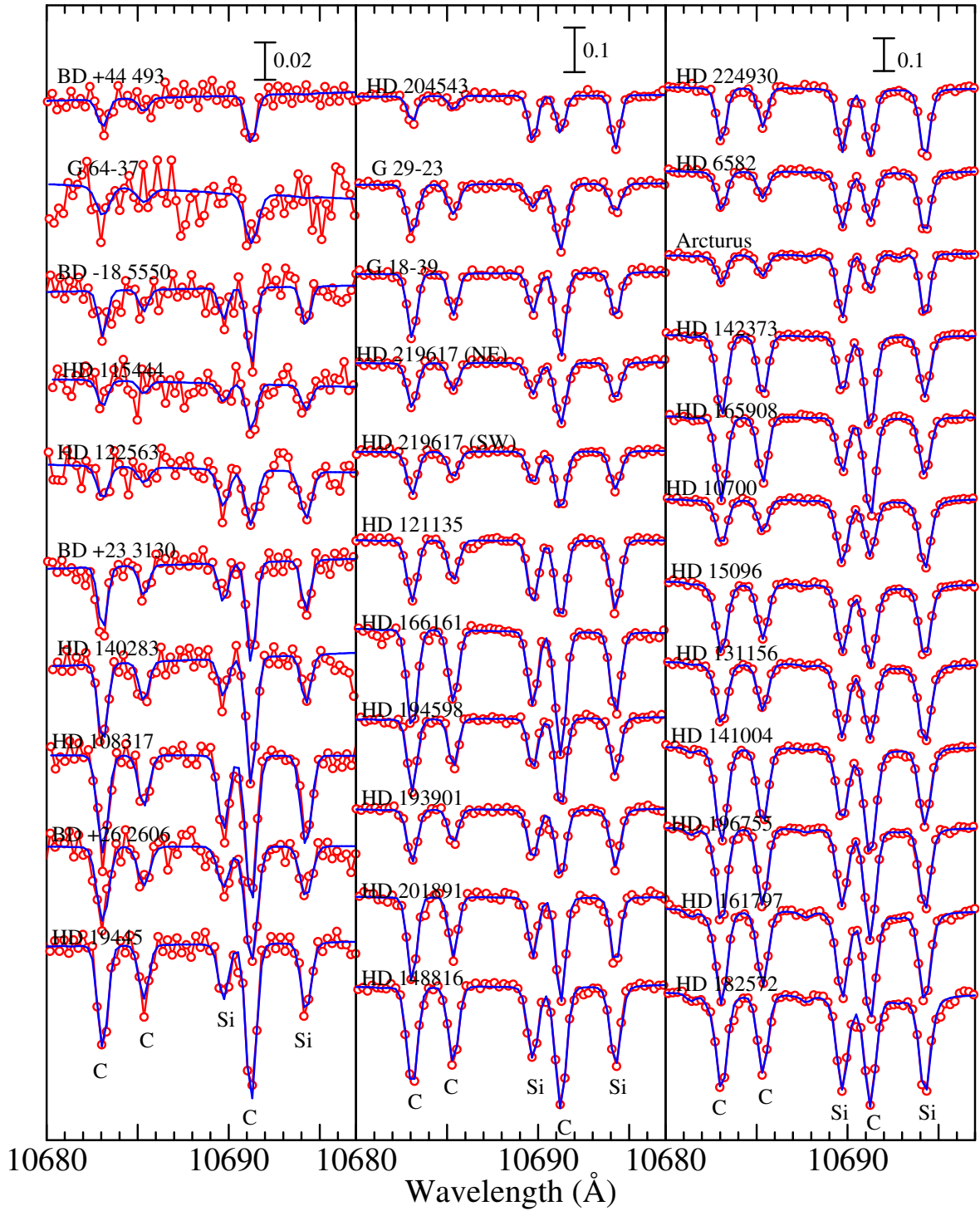


**Fig. 2.** Synthetic spectrum fitting in the 10680–10697 Å region, comprising three C I and two Si I lines, for 33 stars in the wide range of metallicity based on the 2009 July data (cf. Paper I). The best-fit theoretical spectra are shown by (blue) solid lines, while the observed data are plotted by (red) circles. In each panel (from left to right), the spectra are arranged (from top to bottom) in the ascending order of  $[\text{Fe}/\text{H}]$  as in table 1. An appropriate vertical offset (0.05, 0.2, 0.25 for the left, middle, and right panel, respectively) is applied to each spectrum relative to the adjacent one. The wavelength scale of each spectrum is adjusted to the laboratory frame.

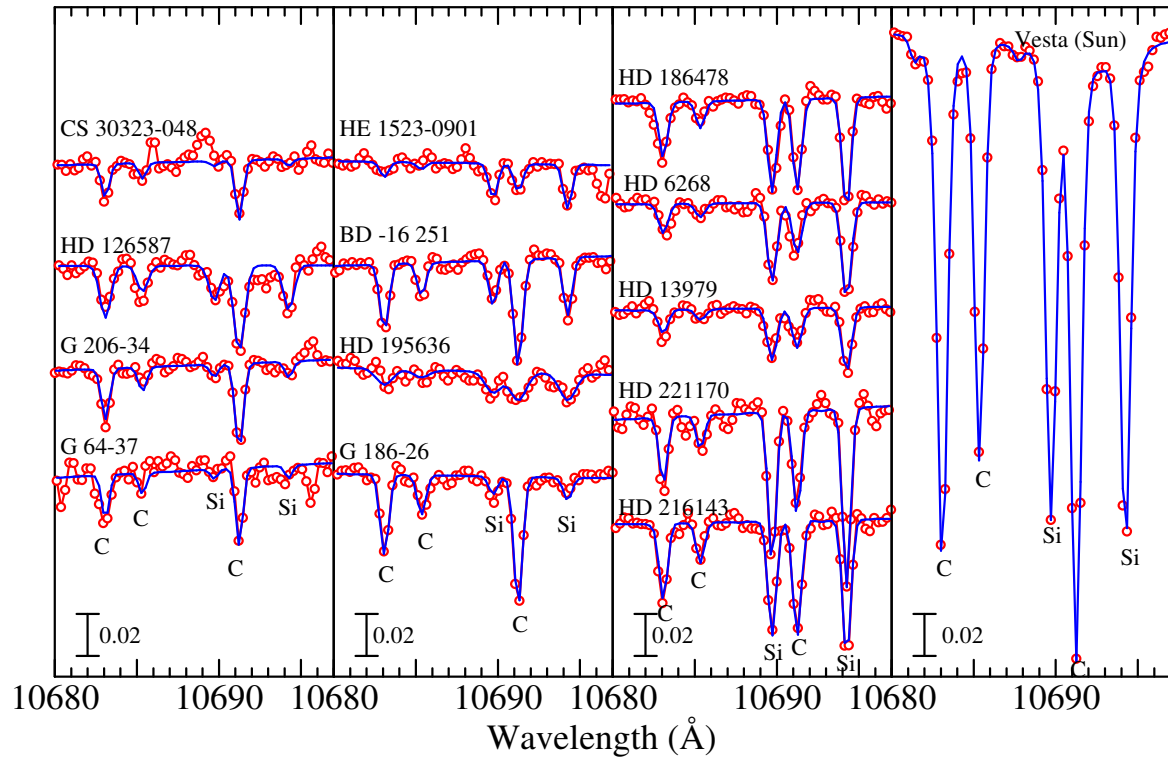


**Fig. 3.** Synthetic spectrum fitting in the 10680–10697 Å region for 12 very metal-poor stars (along with Vesta) based on the 2011 August data (cf. Paper II). The same value (0.05) of vertical offset is applied to each spectrum relative to the adjacent one. Otherwise, the same as in figure 2.

**Table 1.** Parameters of the program stars and the results of the abundance analysis.

Name	$T_{\text{eff}}$ (K)	$\log g$ ( $\text{cm s}^{-2}$ )	$v_t$ ( $\text{km s}^{-1}$ )	[Fe/H] (dex)	$A_{\text{C}}^{\text{N}}$ (dex)	$EW_{10691}$ (mÅ)	$\Delta_{10691}$ (dex)	[C/Fe] (dex)	Remark
(2009 July data)									
BD +44 493	5510	3.70	1.30	−3.68	5.69	19.6	−0.38	+0.83	
G 64-37	6432	4.24	1.50	−3.08	5.64	25.7	−0.29	+0.18	also observed in 2011 August
BD −18 5550	4750	1.40	1.80	−3.06	5.63	26.4	−0.34	+0.15	
HD 115444	4721	1.74	2.00	−2.71	5.64	16.9	−0.24	−0.19	
HD 122563	4572	1.36	2.90	−2.61	5.80	23.7	−0.24	−0.13	
BD +23 3130	5000	2.20	1.40	−2.60	5.99	36.6	−0.28	+0.05	
HD 140283	5830	3.67	1.90	−2.55	6.16	47.0	−0.25	+0.17	
HD 108317	5310	2.77	1.90	−2.35	6.32	60.9	−0.29	+0.13	
BD +26 2606	5875	4.10	0.40	−2.30	6.47	52.3	−0.16	+0.23	
HD 19445	6130	4.39	2.10	−2.05	6.53	62.3	−0.13	+0.04	
HD 204543	4672	1.49	2.00	−1.72	6.39	55.0	−0.25	−0.43	
G 29−23	6194	4.04	1.50	−1.69	6.92	119.8	−0.27	+0.07	
G 18−39	6093	4.19	1.50	−1.46	7.14	131.9	−0.23	+0.06	
HD 219617NE	5825	4.30	1.40	−1.40	7.13	104.5	−0.13	−0.01	North-East component
HD 219617SW	5825	4.30	1.40	−1.40	7.10	101.2	−0.13	−0.04	South-West component
HD 121135	4934	1.91	1.60	−1.37	7.12	133.3	−0.44	−0.05	
HD 166161	5350	2.56	2.25	−1.22	7.42	206.3	−0.57	+0.10	
HD 194598	6020	4.30	1.40	−1.15	7.35	146.0	−0.20	−0.04	
HD 193901	5699	4.42	1.20	−1.10	7.39	118.1	−0.11	−0.05	
HD 201891	5900	4.19	1.40	−1.10	7.53	167.1	−0.23	+0.09	
HD 148816	5860	4.07	1.60	−1.00	7.81	215.3	−0.29	+0.27	
HD 224930	5275	4.10	1.05	−0.90	8.02	153.7	−0.11	+0.38	
HD 6582	5331	4.54	0.73	−0.81	7.88	122.6	−0.06	+0.15	
Arcturus	4281	1.72	1.49	−0.55	8.15	73.0	−0.23	+0.16	
HD 142373	5776	3.83	1.26	−0.51	7.99	228.3	−0.30	−0.04	
HD 165908	6183	4.35	1.24	−0.46	7.96	243.3	−0.25	−0.12	
HD 10700	5420	4.68	0.66	−0.43	8.12	148.3	−0.06	+0.01	
HD 15096	5375	4.30	0.80	−0.20	8.70	246.0	−0.11	+0.36	
HD 131156	5527	4.60	1.10	−0.13	8.41	208.0	−0.09	+0.00	
HD 141004	5877	4.11	1.17	−0.01	8.49	305.0	−0.22	−0.04	
HD 196755	5750	3.83	1.23	0.09	8.45	282.5	−0.26	−0.18	
HD 161797	5580	3.99	1.11	0.29	8.79	302.7	−0.19	−0.04	
HD 182572	5566	4.11	1.07	0.33	8.89	315.2	−0.17	+0.02	
(2011 August data)									
CS 30323-048	6338	4.32	1.50	−3.21	5.52	17.6	−0.28	+0.19	
HD 126587	4700	1.05	1.70	−3.16	5.67	34.5	−0.39	+0.29	
G 206-34	5825	3.99	1.50	−3.12	5.93	27.3	−0.25	+0.51	
G 64-37	6432	4.24	1.50	−3.08	5.57	22.0	−0.28	+0.11	also observed in 2009 July
HE 1523−0901	4630	1.00	2.60	−2.95	5.07	8.9	−0.28	−0.52	
BD −16 251	4825	1.50	1.80	−2.91	5.78	35.6	−0.35	+0.15	
HD 195636	5370	2.40	1.50	−2.77	5.30	16.8	−0.33	−0.47	
G 186-26	6417	4.42	1.50	−2.54	6.11	44.3	−0.19	+0.11	
HD 186478	4730	1.50	1.80	−2.42	5.84	29.7	−0.27	−0.28	
HD 6268	4735	1.61	2.10	−2.30	5.63	17.8	−0.21	−0.61	
HD 13979	5075	1.90	1.30	−2.26	5.34	14.8	−0.23	−0.94	
HD 221170	4560	1.37	1.60	−2.00	6.10	32.4	−0.21	−0.44	
HD 216143	4525	1.77	1.90	−1.92	6.46	37.0	−0.17	−0.16	
Vesta	5780	4.44	1.00	0.00	8.54	283.7	−0.14	+0.00	substitute for the Sun

In columns 1 through 5 are given the star designation, effective temperature, logarithmic surface gravity, microturbulent velocity dispersion, and Fe abundance relative to the Sun, which are the same as adopted in Papers I and II. Columns 6–9 present the results of the abundance analysis.  $A_{\text{C}}^{\text{N}}$  is the non-LTE logarithmic abundance of C (in the usual normalization of  $A_{\text{H}} = 12.00$ ) derived from spectrum-synthesis fitting,  $EW_{10691}$  is the equivalent width (in mÅ) for the C I 10691 line inversely computed from  $A_{\text{C}}^{\text{N}}$ ,  $\Delta_{10691}$  is the non-LTE correction ( $\equiv A_{\text{C}}^{\text{N}} - A_{10691}^{\text{L}}$ ) for the C I 10691 line, and [C/Fe] ( $\equiv A_{\text{C}}^{\text{N}} - 8.54 - [\text{Fe}/\text{H}]$ ) is the C-to-Fe logarithmic abundance ratio relative to the Sun. In each of the two groups corresponding to different observational epochs, the data are arranged in the ascending order of [Fe/H].

**Table 2.** Atomic data of important lines relevant for this study.

Species	RMT	Transition	$\lambda$ (Å)	$\chi_{\text{low}}$ (eV)	$\log gf$	Gammar	Gammas	Gammaw
C I	3	3s $^3P_3^o - 3p$ $^3P_5$	9061.436	7.483	-0.335	(7.43)	-5.32	(-7.59)
C I	3	3s $^3P_3^o - 3p$ $^3P_3$	9078.288	7.483	-0.557	(7.43)	-5.32	(-7.59)
C I	3	3s $^3P_3^o - 3p$ $^3P_1$	9088.513	7.483	-0.432	(7.43)	-5.32	(-7.59)
C I	3	3s $^3P_5^o - 3p$ $^3P_5$	9094.830	7.488	+0.142	(7.43)	-5.32	(-7.59)
C I	3	3s $^3P_5^o - 3p$ $^3P_3$	9111.807	7.488	-0.335	(7.43)	-5.32	(-7.59)
C I	1	3s $^3P_3^o - 3p$ $^3D_5$	10683.083	7.483	+0.076	(7.29)	-5.40	(-7.62)
C I	1	3s $^3P_1^o - 3p$ $^3D_3$	10685.343	7.480	-0.276	(7.29)	-5.40	(-7.62)
C I	1	3s $^3P_5^o - 3p$ $^3D_7$	10691.240	7.488	+0.348	(7.29)	-5.40	(-7.61)
C I	1	3s $^3P_3^o - 3p$ $^3D_3$	10707.317	7.483	-0.401	(7.29)	-5.40	(-7.62)
C I	1	3s $^3P_5^o - 3p$ $^3D_5$	10729.530	7.488	-0.401	(7.29)	-5.40	(-7.62)
Si I	53	4p $^3D_3 - 4d$ $^3F_5^o$	10689.716	5.954	-0.190	(7.29)	-4.23	(-7.29)
Si I	53	4p $^3D_3 - 4d$ $^5F_7^o$	10694.252	5.964	-0.060	(7.29)	-4.23	(-7.29)

All data are were taken from Kurucz and Bell's (1995) compilation as far as available. RMT is the multiplet number given by the Revised Multiplet Table (Moore 1959). In the last three columns are given the damping parameters in the c.g.s. unit: Gammar is the radiation damping constant ( $\text{s}^{-1}$ ),  $\log \gamma_{\text{rad}}$ . Gammas is the Stark damping width per electron density ( $\text{cm}^{-3}$ ) at  $10^4$  K,  $\log(\gamma_e/N_e)$ . Gammaw is the van der Waals damping width per hydrogen density ( $\text{cm}^{-3}$ ) at  $10^4$  K,  $\log(\gamma_w/N_H)$ . Note that the values in parentheses are the default damping parameters computed within the Kurucz's WIDTH program (cf. Leusin, Topil'skaya 1987), because of being unavailable in Kurucz and Bell (1995). The meanings of other columns are self-explanatory.

**Table 3.** Comparison of the [C/H] results and atmospheric parameters with the literature values.

Star	$T_{\text{eff}}$ (K)	$\log g$ ( $\text{cm s}^{-1}$ )	$v_t$ ( $\text{km s}^{-1}$ )	[Fe/H] (dex)	[C/H] (dex)	Ref.	Line
BD +44 493	5510	3.70	1.30	-3.68	-2.85	( <i>this study</i> )	C I 10683/10685/10691
	5510	3.70	1.30	-3.68	-2.37	ITO09	CH (4308–4316)
HD 126587	4700	1.05	1.70	-3.16	-2.87	( <i>this study</i> )	C I 10683/10685/10691
	4960	2.10	1.80	-2.90	-2.59	HON04	CH (4323)
	4910	1.85	2.03	-2.84	-2.71	MCW95	CH ( $\sim$ 4300)
G 64-37	6432	4.24	1.50	-3.08	-2.90	( <i>this study</i> )	C I 10683/10685/10691 [ <i>2009 data</i> ]
	6432	4.24	1.50	-3.08	-2.97	( <i>this study</i> )	C I 10683/10685/10691 [ <i>2011 data</i> ]
	6432	4.24	1.50	-3.08	-3.21	FAB09	C I 9061/9062/9078/9088/9094/9111
	6318	4.16	1.50	-3.12	-2.83	AKE04	C I 9061/9078/9094/9111
BD -18 5550	4750	1.40	1.80	-3.06	-2.91	( <i>this study</i> )	C I 10683/10685/10691
	4750	1.40	1.80	-3.06	-3.08	CAY04	CH (4224)
	4750	1.40	1.80	-3.06	-3.08	SPI05	CH (4224)
	4790	1.15	2.14	-2.91	-2.91	MCW95	CH ( $\sim$ 4300)
	4683	1.70	1.70	-2.87	-3.26	MEL02	CH (4310)
	4750	1.40	1.80	-3.06	-3.08	SPI06	CH (4230)
	4806	1.72	1.91	-2.89	-3.09	JOH07	CH ( $\sim$ 4300)
HD 115444	4721	1.74	2.00	-2.71	-2.90	( <i>this study</i> )	C I 10683/10685/10691
	4720	1.50	1.70	-2.85	-3.26	HON04	CH (4323)
	4775	1.68	2.00	-2.86	-3.01	LAI07	CH ( $\sim$ 4300)
	4721	1.74	2.00	-2.71	-3.45	SIM04	CH (4315)
HD 122563	4572	1.36	2.90	-2.61	-2.74	( <i>this study</i> )	C I 10683/10685/10691
	4600	1.10	2.00	-2.85	-3.22	CAY04	CH (4224)
	4570	1.10	2.20	-2.77	-3.18	HON04	CH (4323)
	4600	1.10	2.00	-2.82	-3.29	SPI05	CH (4224)
	4650	1.40	2.60	-2.68	-3.13	NOR97	CH (4323)
	4600	1.10	2.20	-2.62	-3.02	AOK05	CH (4323)
	4600	1.10	2.00	-2.82	-3.21	SPI06	CH (4230)
	4615	1.27	2.10	-2.47	-3.42	JOH07	CH ( $\sim$ 4300)
	4600	1.10	2.20	-2.58	-2.94	AOK07	CH (4323)
	4610	1.32	2.00	-2.54	-2.94	LAI07	CH ( $\sim$ 4300)
	4572	1.36	2.90	-2.61	-3.32	SIM04	CH (4315)
BD +23 3130	5000	2.20	1.40	-2.60	-2.55	( <i>this study</i> )	C I 10683/10685/10691
	5224	2.82	2.00	-2.59	-2.29	LAI07	CH ( $\sim$ 4300)
	5285	2.83	1.60	-2.62	-2.47	LAI08	CH ( $\sim$ 4300)
HD 140283	5830	3.67	1.90	-2.55	-2.38	( <i>this study</i> )	C I 10683/10685/10691
	5849	3.72	1.50	-2.38	-2.48	FAB09	C I 9061/9062/9078/9088/9094/9111
	5630	3.50	1.40	-2.53	-2.25	HON04	CH (4323)
	5750	3.30	1.20	-2.47	-2.31	AOK02	CH (4323)
	5690	3.69	1.50	-2.42	-2.21	AKE04	C I 9061/9078/9094/9111
	5640	3.28	1.50	-2.64	-2.42	TOM92	C I 9078/9088/9094/9111
	5640	3.28	1.50	-2.64	-2.40	TOM92	CH ( $\sim$ 4300)
G 186-26	6417	4.42	1.50	-2.54	-2.43	( <i>this study</i> )	C I 10683/10685/10691
	6417	4.42	1.50	-2.54	-2.65	FAB09	C I 9061/9062/9078/9088/9094/9111
	6273	4.25	1.50	-2.62	-2.41	AKE04	C I 9061/9078/9094/9111
HD 186478	4730	1.50	1.80	-2.42	-2.70	( <i>this study</i> )	C I 10683/10685/10691
	4700	1.30	2.00	-2.60	-2.92	CAY04	CH (4224)
	4720	1.60	2.20	-2.50	-2.75	HON04	CH (4323)
	4700	1.30	2.00	-2.59	-2.89	SPI05	CH (4224)
	4650	0.95	2.71	-2.58	-2.86	MCW95	CH ( $\sim$ 4300)
	4700	1.30	2.00	-2.59	-2.81	SPI06	CH (4230)
	4831	1.78	1.89	-2.63	-2.83	JOH07	CH ( $\sim$ 4300)
	4598	1.43	2.00	-2.44	-2.96	SIM04	CH (4315)
HD 108317	5310	2.77	1.90	-2.35	-2.22	( <i>this study</i> )	C I 10683/10685/10691
	5234	2.68	2.00	-2.28	-2.23	SIM04	CH (4315)
BD +26 2606	5875	4.10	0.40	-2.30	-2.07	( <i>this study</i> )	C I 10683/10685/10691
	5910	3.63	1.50	-2.63	-2.35	TOM92	C I 9078/9088/9094/9111
	5910	3.63	1.50	-2.63	-2.40	TOM92	CH ( $\sim$ 4300)
HD 6268	4735	1.61	2.10	-2.30	-2.91	( <i>this study</i> )	C I 10683/10685/10691
	4600	1.00	2.10	-2.63	-3.30	HON04	CH (4323)
	4670	0.75	2.73	-2.59	-3.26	MCW95	CH ( $\sim$ 4300)
	4705	1.50	1.90	-2.35	-3.48	MEL02	CH (4310)
HD 13979	5075	1.90	1.30	-2.26	-3.20	( <i>this study</i> )	C I 10683/10685/10691
	4970	1.15	2.35	-2.65	-3.25	MCW95	CH ( $\sim$ 4300)
HD 19445	6130	4.39	2.10	-2.05	-2.01	( <i>this study</i> )	C I 10683/10685/10691
	6047	4.51	0.80	-1.94	-1.99	GRA00	CH (4235, 4365)
	5880	4.40	1.50	-2.15	-1.76	TOM92	C I 9078/9088/9094/9111
	5880	4.40	1.50	-2.15	-2.20	TOM92	CH ( $\sim$ 4300)
HD 221170	4560	1.37	1.60	-2.00	-2.44	( <i>this study</i> )	C I 10683/10685/10691
	4648	1.57	2.22	-2.15	-2.70	BAR05	CH (4310–4313, 4362–4367)
	4460	0.75	1.60	-2.11	-2.41	MEL01	CH ( $\sim$ 4300) [literature value adopted]
	4510	1.00	1.80	-2.20	-2.89	IYA06	CH ( $\sim$ 4300)
	4410	1.09	1.70	-2.03	-2.85	SIM04	CH (4315)
	4648	1.57	2.22	-2.14	-2.71	ZHA11	CH (4310)
	4600	1.50	1.90	-1.98	-2.59	AOK08	CH (4323)
HD 216143	4525	1.77	1.90	-1.92	-2.08	( <i>this study</i> )	C I 10683/10685/10691
	4360	0.50	1.80	-2.22	-2.87	MEL01	CO (1.56 $\mu\text{m}$ , 2.33 $\mu\text{m}$ )
	4450	0.80	2.30	-2.27	-2.64	AOK08	CH (4323)
HD 204543	4672	1.49	2.00	-1.72	-2.15	( <i>this study</i> )	C I 10683/10685/10691

Table 3. (Continued)

Star	$T_{\text{eff}}$ (K)	$\log g$ ( $\text{cm s}^{-1}$ )	$v_t$ ( $\text{km s}^{-1}$ )	[Fe/H] (dex)	[C/H] (dex)	Ref.	Line
	4570	1.24	2.00	-1.98	-2.43	LAI07	CH ( $\sim$ 4300)
	4672	1.49	2.00	-1.72	-2.42	SIM04	CH (4315)
	4600	1.00	2.20	-1.81	-2.44	AOK08	CH (4323)
G 29-23	<i>6194</i>	<i>4.04</i>	<i>1.50</i>	<i>-1.69</i>	<i>-1.62</i>	<i>(this study)</i>	<i>C I 10683/10685/10691</i>
	6194	4.04	1.50	-1.69	-1.91	FAB09	C I 9061/9062/9078/9088/9094/9111
	5966	3.82	1.50	-1.80	-1.70	AKE04	C I 9061/9078/9094/9111
G 18-39	<i>6093</i>	<i>4.19</i>	<i>1.50</i>	<i>-1.46</i>	<i>-1.40</i>	<i>(this study)</i>	<i>C I 10683/10685/10691</i>
	6093	4.19	1.50	-1.46	-1.45	FAB09	C I 9061/9062/9078/9088/9094/9111
	5910	4.09	1.50	-1.52	-1.26	AKE04	C I 9061/9078/9094/9111
HD 219617NE	<i>5825</i>	<i>4.30</i>	<i>1.40</i>	<i>-1.40</i>	<i>-1.41</i>	<i>(this study)</i>	<i>C I 10683/10685/10691</i>
HD 219617SW	<i>5825</i>	<i>4.30</i>	<i>1.40</i>	<i>-1.40</i>	<i>-1.44</i>	<i>(this study)</i>	<i>C I 10683/10685/10691</i>
	5974	3.88	1.23	-1.48	-1.49	GRA00	CH (4235, 4365)
HD 121135	<i>4934</i>	<i>1.91</i>	<i>1.60</i>	<i>-1.37</i>	<i>-1.42</i>	<i>(this study)</i>	<i>C I 10683/10685/10691</i>
	4934	1.91	1.60	-1.37	-1.99	SIM04	CH (4315)
HD 166161	<i>5350</i>	<i>2.56</i>	<i>2.25</i>	<i>-1.22</i>	<i>-1.12</i>	<i>(this study)</i>	<i>C I 10683/10685/10691</i>
	5270	2.51	1.55	-1.08	-1.58	GRA00	CH (4235, 4365)
	5350	2.56	2.25	-1.22	-1.33	SIM04	CH (4315)
HD 194598	<i>6020</i>	<i>4.30</i>	<i>1.40</i>	<i>-1.15</i>	<i>-1.19</i>	<i>(this study)</i>	<i>C I 10683/10685/10691</i>
	6046	4.31	0.80	-1.08	-1.08	GRA00	CH (4235, 4365)
	5906	4.25	1.30	-1.17	-1.07	AKE04	C I 9061/9078/9094/9111
	6044	4.19	1.00	-1.16	-1.13	SIM04	CH (4315)
	5910	4.28	1.50	-1.32	-1.12	TOM92	C I 9078/9088/9094/9111
	5910	4.28	1.50	-1.32	-1.50	TOM92	CH ( $\sim$ 4300)
HD 193901	<i>5699</i>	<i>4.42</i>	<i>1.20</i>	<i>-1.10</i>	<i>-1.15</i>	<i>(this study)</i>	<i>C I 10683/10685/10691</i>
	5823	4.58	0.80	-1.10	-1.21	GRA00	CH (4235, 4365)
	5672	4.38	1.00	-1.12	-1.14	AKE04	C I 9061/9078/9094/9111
	5750	4.46	1.50	-1.16	-1.28	SIM04	CH (4315)
	5810	4.83	1.50	-1.22	-1.26	TOM92	C I 9078/9088/9094/9111
	5810	4.83	1.50	-1.22	-1.90	TOM92	CH ( $\sim$ 4300)
HD 201891	<i>5900</i>	<i>4.19</i>	<i>1.40</i>	<i>-1.10</i>	<i>-1.01</i>	<i>(this study)</i>	<i>C I 10683/10685/10691</i>
	5991	4.30	1.10	-1.13	-0.92	GRA00	CH (4235, 4365)
	5909	4.19	1.00	-1.10	-1.04	SIM04	CH (4315)
HD 148816	<i>5860</i>	<i>4.07</i>	<i>1.60</i>	<i>-1.00</i>	<i>-0.73</i>	<i>(this study)</i>	<i>C I 10683/10685/10691</i>
	5823	4.14	1.20	-0.73	-0.53	AKE04	C I 9061/9078/9094/9111
HD 6582	<i>5331</i>	<i>4.54</i>	<i>0.73</i>	<i>-0.81</i>	<i>-0.66</i>	<i>(this study)</i>	<i>C I 10683/10685/10691</i>
	5408	4.40	0.80	-0.83	-0.79	MEL01	CO (1.56 $\mu\text{m}$ , 2.33 $\mu\text{m}$ )
Arcturus	<i>4281</i>	<i>1.72</i>	<i>1.49</i>	<i>-0.55</i>	<i>-0.39</i>	<i>(this study)</i>	<i>C I 10683/10685/10691</i>
	4350	1.80	1.70	-0.51	-0.67	KJA82	C <sub>2</sub> (5630)
	4286	1.66	1.74	-0.52	-0.09	RAM11	C I 5380/8335/9078/9111
HD 142373	<i>5776</i>	<i>3.83</i>	<i>1.26</i>	<i>-0.51</i>	<i>-0.55</i>	<i>(this study)</i>	<i>C I 10683/10685/10691</i>
	5776	3.83	1.26	-0.51	-0.38	TAK05	C I 5052/5380
HD 165908	<i>6183</i>	<i>4.35</i>	<i>1.24</i>	<i>-0.46</i>	<i>-0.58</i>	<i>(this study)</i>	<i>C I 10683/10685/10691</i>
	6183	4.35	1.24	-0.46	-0.24	TAK05	C I 5052/5380
HD 10700	<i>5420</i>	<i>4.68</i>	<i>0.66</i>	<i>-0.43</i>	<i>-0.42</i>	<i>(this study)</i>	<i>C I 10683/10685/10691</i>
	5420	4.68	0.66	-0.43	-0.20	TAK05	C I 5052/5380
HD 131156	<i>5527</i>	<i>4.60</i>	<i>1.10</i>	<i>-0.13</i>	<i>-0.13</i>	<i>(this study)</i>	<i>C I 10683/10685/10691</i>
	5527	4.60	1.10	-0.13	-0.14	TAK05	C I 5052/5380
HD 141004	<i>5877</i>	<i>4.11</i>	<i>1.17</i>	<i>-0.01</i>	<i>-0.05</i>	<i>(this study)</i>	<i>C I 10683/10685/10691</i>
	5877	4.11	1.17	-0.01	0.02	TAK05	C I 5052/5380
HD 196755	<i>5750</i>	<i>3.83</i>	<i>1.23</i>	<i>0.09</i>	<i>-0.09</i>	<i>(this study)</i>	<i>C I 10683/10685/10691</i>
	5750	3.83	1.23	0.09	-0.05	TAK05	C I 5052/5380
HD 161797	<i>5580</i>	<i>3.99</i>	<i>1.11</i>	<i>0.29</i>	<i>0.25</i>	<i>(this study)</i>	<i>C I 10683/10685/10691</i>
	5580	3.99	1.11	0.29	0.27	TAK05	C I 5052/5380
HD 182572	<i>5566</i>	<i>4.11</i>	<i>1.07</i>	<i>0.33</i>	<i>0.35</i>	<i>(this study)</i>	<i>C I 10683/10685/10691</i>
	5566	4.11	1.07	0.33	0.39	TAK05	C I 5052/5380

For the metal-poor objects with  $[\text{Fe}/\text{H}] \lesssim -0.8$  (i.e., from BD +44 493 through HD 6582), we consulted the SAGA database (Suda et al. 2008, 2011) as of the end of 2012 November, in which the  $[\text{C}/\text{H}]$  values are reduced to the reference solar carbon abundance of 8.55 (Grevesse et al. 1996). In addition, we also included  $[\text{C}/\text{H}]$  values from two papers which were missing in SAGA: 5 stars (HD 19445, HD 140283, HD 193901, HD 194598, BD +26 2606) from Tomkin et al. (1992) and 5 stars (G 64-37, HD 140283, G 29-23, G 18-39, G 186-26) from Fabbian et al. (2009; results for the  $S_{\text{H}} = 1$  case were adopted and renormalized to the solar abundance of 8.55). Meanwhile, regarding stars of  $[\text{Fe}/\text{H}] \gtrsim -0.5$  (i.e., from Arcturus through HD 182572) where SAGA does not cover, the data were taken from Kjaergaard et al. (1982) and Ramírez et al. (2011) for Arcturus, as well as from Takeda and Honda (2005) for the other disk stars (an extensive literature survey has not been performed for those non-SAGA stars). The reference source is given in the 7th column, and the adopted lines used for C-abundance determination are also noted in the 8th column. Our data adopted/derived in this study are expressed in italic. Stars are arranged in the ascending order of  $[\text{Fe}/\text{H}]$  (the metallicity value adopted in this study).

Key to the references: AKE04 — Akerman et al. (2004); AOK02 — Aoki et al. (2002); AOK05 — Aoki et al. (2005); AOK07 — Aoki et al. (2007); AOK08 — Aoki and Honda (2008); BAR05 — Barklem et al. (2005); CAY04 — Cayrel et al. (2004); FAB09 — Fabbian et al. (2009); GRA00 — Gratton et al. (2000); HON04 — Honda et al. (2004); ITO09 — Ito et al. (2009); IVA06 — Ivans et al. (2006); JOH07 — Johnson et al. (2007); KJA82 — Kjaergaard et al. (1982); LAI07 — Lai et al. (2007); LAI08 — Lai et al. (2008); MCW95 — McWilliam et al. (1995); MEL01 — Meléndez, Barbuy, and Spite (2001); MEL02 — Meléndez and Barbuy (2002); NOR97 — Norris, Ryan, and Beers (1997); RAM11 — Ramírez and Allende Prieto (2011); SIM04 — Simmerer et al. (2004); SPI05 — Spite et al. (2005); SPI06 — Spite et al. (2006); TAK05 — Takeda and Honda (2005); TOM92 — Tomkin et al. (1992); ZHA11 — Zhang et al. (2011).